Flow dynamics of the resonances of a two-dimensional circular quantum well

Meeten, R.P.; Docherty-Walthew, G.S.; Morozov, G.V.

Published in:
Physical Review A

DOI:
10.1103/PhysRevA.99.042126

Published: 29/04/2019

Flow dynamics of the resonances of a 2D circular quantum well

R. P. Meeten[1], G. S. Docherty-Walthew[1,2], and G. V. Morozov[1*]
[1] *Scottish Universities Physics Alliance (SUPA), Institute of Thin Films, Sensors and Imaging, University of the West of Scotland, Paisley PA1 2BE, United Kingdom*
[2] *Scottish Universities Physics Alliance (SUPA), School of Physics and Astronomy, University of St. Andrews, St. Andrews KY16 9SS, United Kingdom*
(Dated: April 3, 2019)

Bound states and resonances are physically important solutions of the time-independent Schrodinger equation for a given quantum mechanical potential. One can find these states using numerical analysis techniques by searching for poles in the scattering amplitude, or equivalently by locating the zeros of particular transcendental, complex-valued functions. We show that the evolution of these solutions displays much deeper behavior than one may assume when parameters of the potential are varied, giving insight into the relationship between different types of solution.

PACS numbers: 03.65.w, 42.25.p, 02.30.Gp, 05.45.Mt

I. INTRODUCTION

The complex wavenumber plane is a rich mathematical structure, and a rather elegant way to represent the various types of solutions of the time independent Schrodinger equation for quantum mechanical potentials. This is because it allows the bound states and resonances of such potentials to be displayed together in a natural way, and shows the interplay between them. The level dynamics of bound states and resonances for one-dimensional (1D) potentials are studied in Refs. [1–4]. In particular, using the square well potential as an example, it was calculated how these states move around in the complex wavenumber plane as the potential depth is increased. The trajectories traced out as the states move around the complex plane are known as *flows*.

Resonances are ubiquitous throughout all of physics, arising in mechanical, optical, quantum mechanical and gravitating systems. Moreover, the importance of the phenomenon of resonance in modern technology is hard to overstate. This is, in particular, due to significant progress in the field of semiconductor nanostructures, microcavity lasers, and biosensing. For theoretical purposes, it is especially useful to know the complete set of all possible resonances for a particular quantum mechanical system for every combination of the potential parameters, as this facilitates the use of techniques such as the resonant state expansion method, see Ref. [5]. More broadly, owing to the global importance of resonance effects, the ability to fully elucidate the evolution of resonances for any physical system in response to variation of that system's parameters will be of great utility.

In this work, we study the level dynamics of the bound states and resonances of two-dimensional (2D) potentials, using a circular finite well as an example. Bound states have real energy eigenvalues and lie mostly inside the well, while resonances have complex energy eigenvalues and lie mostly outside the well. Possible states of a circular infinite well were investigated in Refs. [6, 7]. Here, we calculate the flows of a circular finite well as a function of its depth. We found that the mechanism by which bound states are created beginning with a potential of effectively zero depth has an interesting interpretation in terms of the resonance-antiresonance pairs - that the bound states can in some sense be considered as a result of the convergence of the corresponding flows to the positive imaginary axis. We also observe resonances which never become bound states. In this regard we classify resonances into two sets: those which lead to the generation of new bound states, and those which converge asymptotically to a complex limit. Following the common terminology, see Refs. [8, 9], we will call the first set "internal" resonances and the second set "external" ("shape") resonances. In the context of 2D optical microdisks, the behavior of internal and external resonances were studied in detail in Refs. [10–12], see also Ref. [13] for a general review. This paper, to the best of our knowledge, is the first complete treatment of the behavior of complex eigenvalues, including the internal and external resonances as well as the bound states, of the 2D Hamiltonian corresponding to a circular finite well.

II. PROPERTIES OF RESONANT STATES

The coordinate parts $\psi_n(\mathbf{r})$ of the resonant state wave functions $\Psi_n(\mathbf{r},t)$ are the eigensolutions of the time-independent Schrodinger equation

$$\left[-\nabla^2 + V(\mathbf{r})\right]\psi_n(\mathbf{r}) = k_n^2\psi_n(\mathbf{r}), \tag{1}$$

subject to the outgoing wave boundary condition. For brevity of notation we used the units $\hbar = 1$ and $\mu = 1/2$, where μ is the particle mass, and for further convenience we introduced the wavenumber k_n of the resonant state, which we simply call the resonance, related to the eigenvalue of the resonant state as

$$\mathcal{E}_n = k_n^2. \tag{2}$$

*Electronic address: gregory.morozov@uws.ac.uk

For 2D problems the outgoing wave boundary condition takes the form

$$\psi_n(\mathbf{r}) \to \frac{\exp(ik_n r)}{\sqrt{r}}, \quad r \to \infty, \tag{3}$$

where $r = |\mathbf{r}|$.

Solving Eqs. (1-2) with the boundary conditions given by Eq. (3), one arrives at the fact that the eigenvalues $\mathcal{E}_n$ are in general complex-valued numbers, often called the complex-valued energies, with real and imaginary parts being the resonance energy E_n and the resonance width Γ_n respectively, i.e.

$$\mathcal{E}_n = E_n - \frac{1}{2}\, i\, \Gamma_n, \quad \Gamma_n > 0. \tag{4}$$

The (time-dependent) resonant state wave functions, $\Psi_n(\mathbf{r}, t)$, are then

$$\Psi_n(\mathbf{r}, t) = \psi_n(\mathbf{r}) \exp(-iE_n t) \exp(-\Gamma_n/2\, t). \tag{5}$$

In terms of the corresponding wavenumbers k_n, the complex-valued energies are expressed as

$$\mathcal{E}_n = [\mathrm{Re}(k_n) + i\, \mathrm{Im}(k_n)]^2. \tag{6}$$

The bound states are then the states with $\mathrm{Re}(k_n) = 0$ and $\mathrm{Im}(k_n) > 0$. Their energies are real negative and their wave functions ψ_n vanish far from the potential. For antibound states, if they exist, see Ref. [14], $\mathrm{Re}(k_n) = 0$ and $\mathrm{Im}(k_n) < 0$, the wave functions ψ_n are purely growing waves outside of the potential, even though their energies are still real and negative. All resonant states with $\mathrm{Re}(k_n) \neq 0$ have $\mathrm{Im}(k_n) < 0$. Their energies are complex-valued numbers and their wave functions $\psi_n(\mathbf{r})$ oscillate and grow exponentially outside the potential.

Time reversal invariance requires that if $\Psi_n(\mathbf{r}, t)$ with the complex-valued energy $\mathcal{E}_n$ is a solution of the time-dependent Schrodinger equation, then $\Psi_n^*(\mathbf{r}, -t)$ with the complex-valued energy $\mathcal{E}_n^*$ should also be a solution of the same equation. In terms of the coordinate parts of the resonant wave functions $\psi_n(\mathbf{r})$ and the corresponding resonant wavenumbers k_n, this means that if $\psi_n(\mathbf{r})$ with $k_n = \mathrm{Re}(k_n) + i\, \mathrm{Im}(k_n)$ satisfies Eqs. (1-3), then $\psi_n^*(\mathbf{r})$ with $\tilde{k}_n = -\mathrm{Re}(k_n) + i\, \mathrm{Im}(k_n)$ should also satisfy the same equations. These states with negative real part are henceforth referred to as antiresonances.

III. RESONANCE CONDITION

The finite circular potential well is described by

$$V(\mathbf{r}) = \begin{cases} -V_0, & r < R, \\ 0, & r > R, \end{cases} \tag{7}$$

where V_0 is the depth of the well (positive number), and R is the radius of the well. The natural geometry of the problem suggests the use of polar coordinates (r, φ). The time-independent Schrodinger equation (1) reduces to

$$\begin{aligned} &\frac{\partial^2\psi}{\partial r^2} + \frac{1}{r}\frac{\partial\psi}{\partial r} + \frac{1}{r^2}\frac{\partial^2\psi}{\partial\varphi^2} + \kappa^2\psi(r,\varphi) = 0, \quad r < R, \\ &\frac{\partial^2\psi}{\partial r^2} + \frac{1}{r}\frac{\partial\psi}{\partial r} + \frac{1}{r^2}\frac{\partial^2\psi}{\partial\varphi^2} + k^2\psi(r,\varphi) = 0, \quad r > R, \end{aligned} \tag{8}$$

where

$$\kappa = \sqrt{k^2 + V_0}. \tag{9}$$

At the boundary of the well, $r = R$, the wave function ψ and its derivative have to be continuous. Moreover, for physical reasons the value of the wave function at the well center must be finite. These boundary conditions together with the outgoing condition given by Eq. (3) define the resonant wave functions in the form of the 'whispering gallery' (WG) modes, given as

$$\psi_m = \begin{cases} N_m J_m(\kappa r) \begin{pmatrix} \cos m\varphi \\ \sin m\varphi \end{pmatrix}, & r < R, \\ \\ H_m(kr) \begin{pmatrix} \cos m\varphi \\ \sin m\varphi \end{pmatrix}, & r > R, \end{cases} \tag{10}$$

where the complex-valued wavenumbers k_n (resonances) of the resonant states satisfy the system of transcendental equations

$$\begin{cases} N_m J_m(\kappa R) - H_m(kR) = 0, \\ \kappa\, N_m J_m^{'}(\kappa R) - k\, H_m^{'}(kR) = 0. \end{cases} \tag{11}$$

Here J_m and H_m are Bessel and Hankel functions of the first kind respectively and $m = 0, 1, 2, ...$ is the angular quantum number. The constants N_m are given by

$$N_m = H_m(kR)/J_m(\kappa R). \tag{12}$$

The angular quantum number $m = 0, 1, 2, \ldots$ characterizes the resonant wave function variation along the azimuthal direction, with the number of intensity hotspots being equal to $2m$. The resonances, k_n, are twofold degenerate for $m > 0$, and nondegenerate for $m = 0$. For each $m > 0$ there are infinitely many internal resonances and a finite number of external/shape resonances, see Refs. [10, 15]. Then, the radial quantum numbers $q_i = 1, 2, \ldots$ and $q_e = 1, 2, \ldots, Q$, where Q is a finite positive integer, will be used to label different internal and external resonances within the group of resonances with the same angular quantum number m, in accordance with increasing real parts of the wavenumbers. Thus, the above overall quantum number n includes for the problem at hand two physical quantum numbers: either m and q_i, or m and q_e. For the internal resonances which are relatively close to the real axis of the complex wavenumber plane the radial quantum number q_i gives in general the number of intensity spots in the radial direction.

Further, it follows immediately from Eqs. (11) that the resonances k_n are solutions of the transcendental equation

$$k\, J_m(\kappa R) H_m^{'}(kR) - \kappa\, J_m^{'}(\kappa R) H_m(kR) = 0. \qquad (13)$$

The Hankel function $H_m(z)$ is a multiple-valued function, which can be represented, see Refs. [16, 17], as

$$H_m(z) = J_m(z) + i\, S_m(z) + i\, \frac{2}{\pi} J_m(z) \ln\left(\frac{z}{2}\right). \qquad (14)$$

Here $J_m(z)$ is a Bessel (single-valued) function, $S_m(z)$ is a single-valued polynomial given by

$$\begin{aligned} S_m(z) = &-\frac{1}{\pi} \sum_{j=0}^{m-1} \frac{(m-j-1)!}{j!} \left(\frac{z}{2}\right)^{2j-m} \\ &- \frac{1}{\pi} \sum_{j=0}^{\infty} (-1)^j \frac{1}{j!(j+m)!} \left(\frac{z}{2}\right)^{m+2j} \\ &\times \left[F(j+1) + F(j+m+1) \right], \end{aligned} \qquad (15)$$

where $F(x)$ is the digamma function defined as the logarithmic derivative of the gamma function $\Gamma(x)$ in accordance with

$$F(x) = \frac{d \ln \Gamma(x)}{dx}, \qquad (16)$$

while the function $\ln(z)$ is a multiple-valued function defined on an infinite number of Riemann sheets. However, only one of those sheets provides the asymptotics for the Hankel function $H_m(z)$ given by Eq. (3). This physical sheet has a cut going from the branch point at $z = 0$ to infinity, and the standard approach is to place the cut on the negative real axis, i.e. define a single-valued function $\ln(z)$ with the modulus r and the argument ϕ as

$$\ln(z) = \ln(r) + i\phi, \quad -\pi < \phi \le \pi. \qquad (17)$$

But such a choice destroys the time-reversal symmetry of resonances across the negative imaginary axis, see the last paragraph of the previous section. In order to keep that symmetry, the cut needs to be moved to the negative imaginary axis as discussed in Ref. [18]. This can be done by redefining the argument of the function $\ln(z)$ in Eq. (17) in accordance with

$$\begin{aligned} &\phi \to \phi, && -\pi/2 < \phi \le \pi, \\ &\phi \to \phi + 2\pi, && -\pi < \phi \le -\pi/2\,. \end{aligned} \qquad (18)$$

As a result, the modified (branch cut placed on the negative imaginary axis) Hankel function will have different values from the original (branch cut placed on the negative real axis) function in the third quadrant, preserving the required symmetry, i.e. fulfilling the condition

$$[H_m(-z^*)]^* = H_m(z). \qquad (19)$$

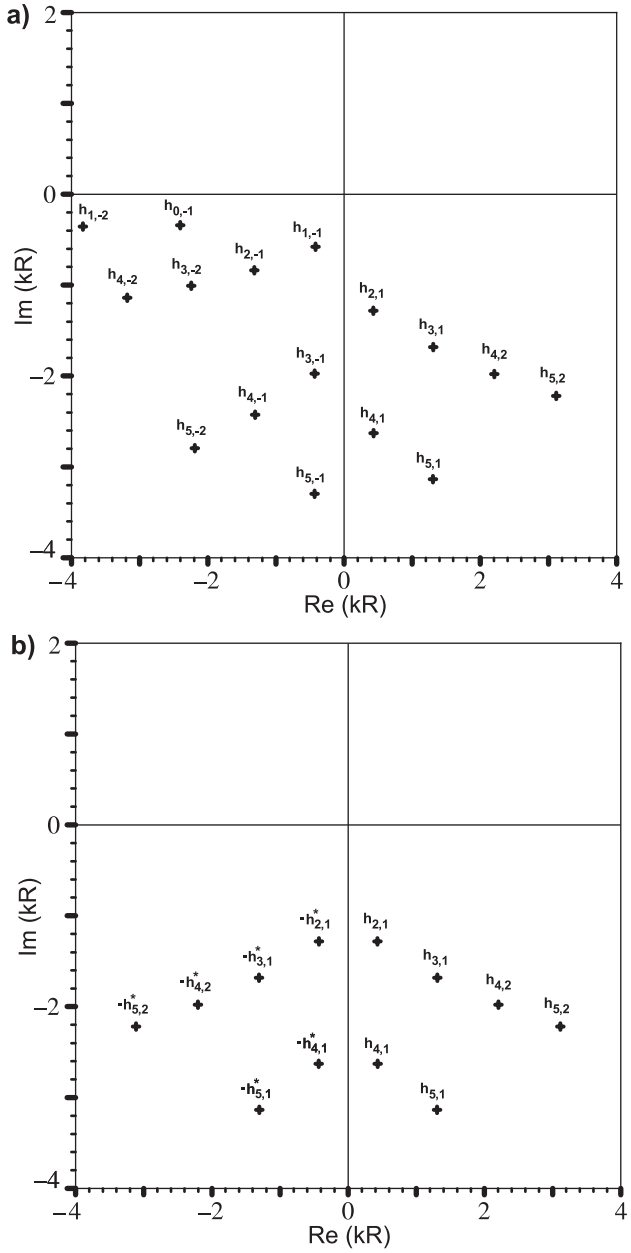

FIG. 1: The locations of complex zeros h_{m,q_e} of the Hankel functions $H_m(kR)$ with the (original) branch cut on the negative real axis [upper panel] and with the (modified) branch cut on the negative imaginary axis [lower panel].

Now, using the standard identities for the derivatives of Bessel and Hankel functions, see Refs. [16, 17], we can rewrite Eq. (13) as

$$k\, J_m(\kappa R) H_{m+1}^{(1)}(kR) - \kappa J_{m+1}(\kappa R) H_m^{(1)}(kR) = 0. \qquad (20)$$

This equation with the modified (branch cut placed on the negative imaginary axis) Hankel functions fulfilling the required symmetry given by Eq. (19) is the resonance condition we analyze. For particular potential depths, V_0, and potential radii, R, it can be solved numerically

to obtain the resonances and bound states of a circular finite well.

If the asymptotics of Eq. (20) are studied for $V_0 \to \infty$, it becomes apparent that the limiting behavior of the external resonances, for which $q_e \leq Q$, is controlled by the zeros of the Hankel functions of order m. The limiting behavior of the internal resonances is influenced by the locations of the zeros of Bessel functions, which are real numbers. When the potential depth exceeds some critical value, these real zeros eventually result in purely imaginary values for kR, which are bound states.

The distribution of complex zeros h_{m,q_e}, which has no symmetry for the Hankel functions with the original cut, see Refs. [19, 20], becomes symmetric with respect to the negative imaginary axis for the Hankel functions with the modified branch cut, see Fig. 1. It is known, see Ref. [21], that there is only a finite number of such zeros for a given m, which correspond to the number of external resonances, Q, for that m. In the fourth quadrant of the complex kR plane, the Hankel functions with the original cut, or in both the third and fourth quadrants, the Hankel functions with the modified cut, the number of external resonances for a given m is $Q = 0$ if $m = 0, 1$, $Q = m/2$ if m is even, and, finally, $Q = (m-1)/2$ if m is odd.

IV. RESONANCE FLOWS

In this work, a method originally due to Wagon, see Ref. [22], was adapted such that the complex equation $f(z) = 0$ is viewed from the vantage of the real system, i.e. given that $f(z) = u(x, y) + iv(x, y)$, one must solve the system

$$\begin{cases} u(x, y) = 0, \\ v(x, y) = 0. \end{cases} \tag{21}$$

The zero level curves of one of these functions are then plotted, and for every point along these curves, the sign of the other function is tested. Where there is a sign change, this corresponds to an approximate position where both $u(x, y) = 0$ and $v(x, y) = 0$, and is thus a crude approximation to a complex root. These initial "seeds" can be fed into a root-finding algorithm such as the Newton-Raphson method, and should converge rapidly to the actual root, since the initial approximation will be reasonably close to the true root. An example output of this method is shown in Fig. 2.

It should be noted that the method illustrated in Fig. 2 appears to show extra crossings of the zero levels which we have not included as physical states. The rationale for this is that although these points are solutions of the transcendental resonance condition given by Eqs. (19, 20), they are **not** solutions of the original system of transcendental equations, see Eq. (11), which arises from boundary conditions. They are acquired when recasting the original system as a single transcendental equation. These *extraneous* solutions occur on the imaginary axis at $kR = \pm i\sqrt{V_0}$, and are filtered out in the numerical procedure.

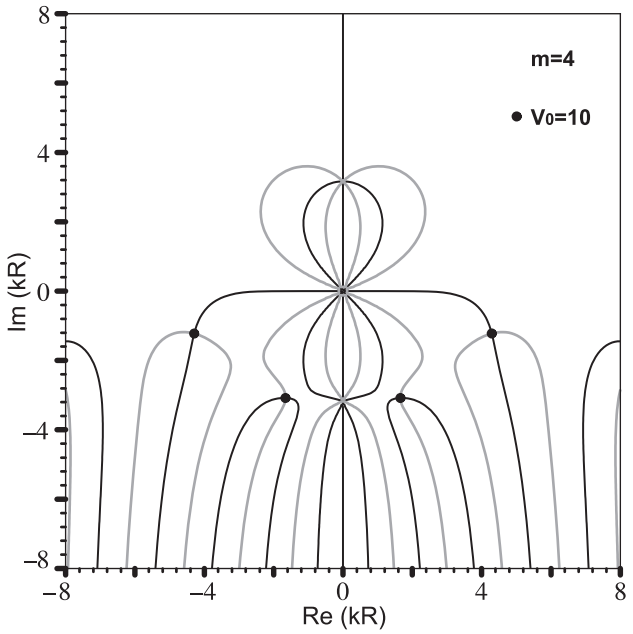

FIG. 2: Wagon's method applied to the case $m = 4$ for a circular well of $V_0 = 10$. The grey (black) lines indicate where the imaginary (real) part of the resonance condition Eq. (15) vanishes. Their intersection represents a complex root of the resonance condition, and is indicated by a black point. Note the removal of the extraneous solutions at $kR = \pm i\sqrt{10}$.

It can be fruitful to see how these resonances vary as a function of the potential depth. The trajectory traced out by incrementally varying the potential depth and following one resonance is known as the flow of that resonance. What results is some truly surprising dynamical richness, complete with attractors and cycles, as well as a clear picture of the interplay and conversion between resonances and bound states.

When analyzing the data, three cases emerge. The special case $m = 0$, and the cases where $m > 0$ is even or odd. Two types of flows also become apparent. The external, or "shape" type flows result in spirals which asymptotically approach zeros of Hankel functions, and internal type flows which are responsible for the generation of new bound states from resonances in the continuum.

The number and location of zeros of Hankel functions seem to be the key features that determine the flow behavior. In all cases, these zeros play the role of attractors in the parlance of dynamical systems theory. The reason for the aforementioned three cases stems from the fact that the relevant Hankel functions have different distributions of zeros for each case. Each zero, or attractor, appears to be "used up" after influencing a flow, in that each zero only alters the trajectory of a single flow.

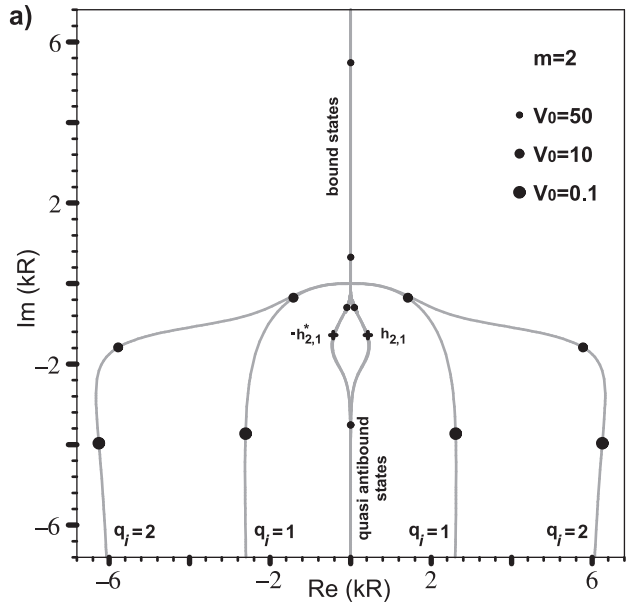

FIG. 3: Flows of the resonances and antiresonances, shown in grey, of a 2D circular well of radius R and potential V_0 in the complex kR plane, as V_0 is deepened beginning from effectively zero depth, for values of $m = 2$ [upper panel] and $m = 4$ [lower panel]. The labels q_i (q_e) denote internal (external) flows respectively. Each pair of doubly degenerate internal resonance-antiresonance flows produces a doubly degenerate bound state flow and two symmetrical non-degenerate quasi antibound state flows.

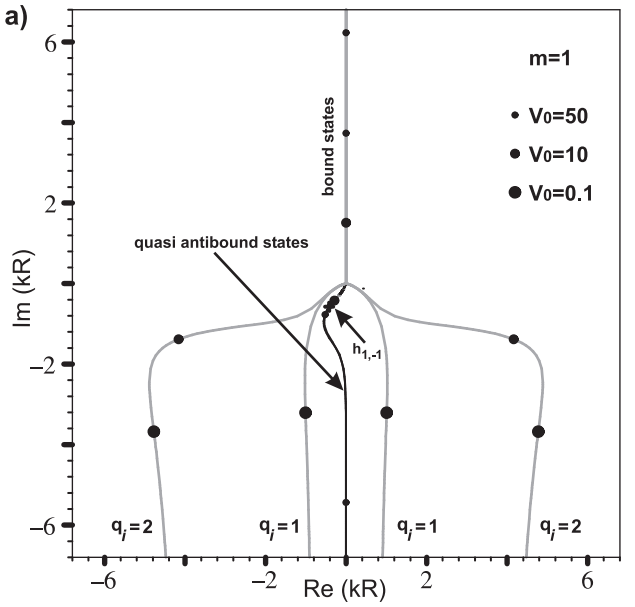

FIG. 4: Flows of the resonances and antiresonances, shown in grey, of a 2D circular well of radius R and potential V_0 in the complex kR plane, as V_0 is deepened beginning from effectively zero depth, for values of $m = 1$ [upper panel] and $m = 3$ [lower panel]. The labels q_i (q_e) denote internal (external) flows respectively. Each pair of the doubly degenerate internal resonance-antiresonance flows produces a doubly degenerate bound state flow and a doubly degenerate quasi antibound state flow (black) from the adjacent branch.

A. Even $m > 0$

The full flow portrait is symmetric across the imaginary axis, indicating that time-reversal symmetry now appears naturally. For these resonances, only the principal branch of the modified resonance condition, see Eqs. (19, 20), is needed as the number of states is conserved, provided that degeneracies are taken into account, i.e. that all state flows in Fig. 3, with the exception of split antibound state flows, see below, are doubly degenerate. The interesting and unusual feature of these flows is in their splitting when a new bound state is generated. To ensure the number of states is conserved, it is supposed that every time a new doubly degenerate bound

state is created in coincidence with the generation of a resonance-antiresonance pair very close to the negative imaginary axis, these "quasi antibound" states (states which resemble antibound states, but have small, non-zero real part) are pulled away from one another by the attractor character of Hankel function zeros. The quasi antibound states then appear to recombine asymptotically as their flows move away from the Hankel zeros. Note that those quasi antibound state flows in Fig. 3 are actually two flows close together, with one corresponding to each created bound state: one from the pair of resonance-antiresonance flows with $q_i = 1$ and one from the pair of resonance-antiresonance flows with $q_i = 2$. The symmetry in this case accords with the symmetric distribution of zeros of the modified Hankel function about the imaginary axis, as shown in Fig. 1b.

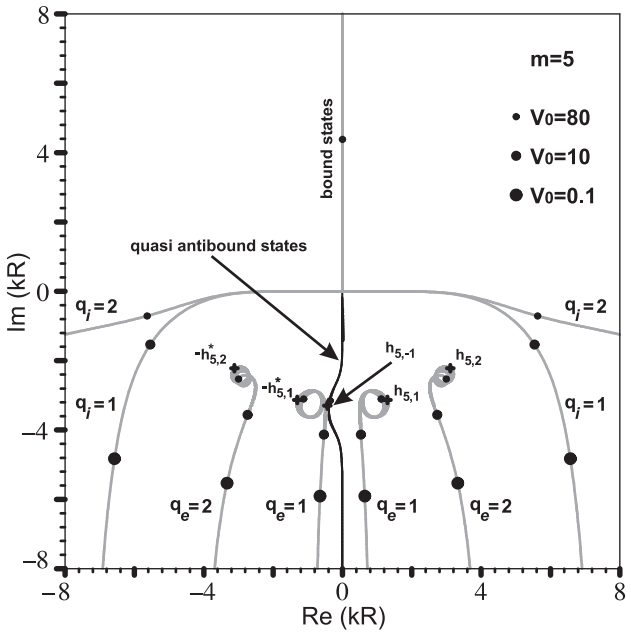

FIG. 5: Same as Fig. 4 but for $m = 5$.

B. Odd $m > 0$

In this case there is an additional complication. While it is apparent that the internal flows are time-reversal symmetric, their coalescence into a new bound state poses a problem. The number of states is no longer conserved if we consider only the principal branch of the modified resonance condition, see again Eqs. (19, 20). Each flow is doubly degenerate and produces a doubly degenerate bound state, which means there are always two states missing as required by state conservation when a new bound state is manifest. This problem can be resolved by augmenting the set of solutions of the resonance condition with additional antiresonance (quasi antibound state) flows which are located in the adjacent branch and appear upon creation of new bound states, as shown in Figs. 4, 5 as a black flow. Note that these figures actually show two such flows which almost coincide: one upon creation of the bound state from the pair of resonance-antiresonance flows with $q_i = 1$ and one upon creation of the bound state from the pair of resonance-antiresonance flows with $q_i = 2$. We suppose that these supplementary flows must be doubly degenerate to address the problem of non-conservation. The addition of such flows is also motivated by the presence of the analogous flows in the even case. The difference here is that while these flows occur as non-degenerate pairs in the even case, as shown in Fig. 3, the lack of symmetric partner flows dictates that they must now be doubly degenerate in this case. This is consistent with the asymmetric distribution of attracting zeros of the original Hankel function, shown in Fig. 1a. This hypothesis can be tested by perturbing the symmetry of the potential with point scatterers, breaking the degeneracy. If the multiplicities assigned to these states are correct, the number of flows arising from the unperturbed cases should be predictable.

C. Special case $m = 0$

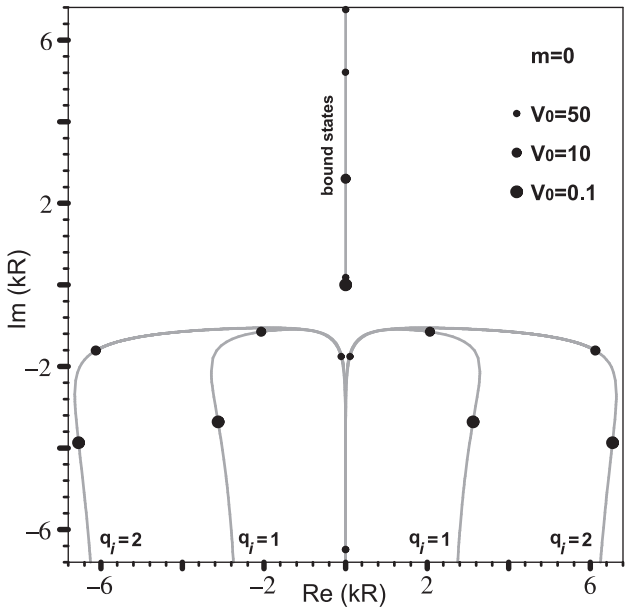

FIG. 6: Flows of the resonances and antiresonances, shown in grey, of a 2D circular well of radius R and potential V_0 in the complex kR plane, as V_0 is deepened beginning from effectively zero depth, for $m = 0$. Note the absence of any split flows or spirals which agrees with the non-existence of the modified Hankel function $H_0(z)$ zeros.

This case, see Fig. 6, immediately distinguishes itself as unique. The mechanism for creating bound states is different, in that there is no splitting of the flows into two parts. Instead, the bound state is created from the origin when resonance-antiresonance flow pairs approach one another within some tolerance. The time-reversal

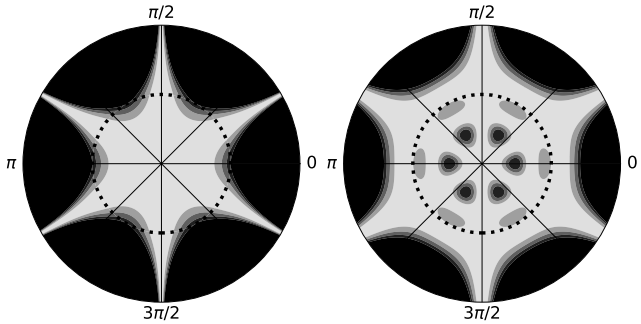

FIG. 7: The probability density $|\psi_n(\mathbf{r})|^2$ for the first external resonance with $m = 3$ and $q_e = 1$, see Fig. 4b, flow $q_e = 1$: $V_0 = 10$ [left panel] and $V_0 = 80$ [right panel]. High (low) density shown as dark (light). Black dotted ring at $r = 1$ is well boundary.

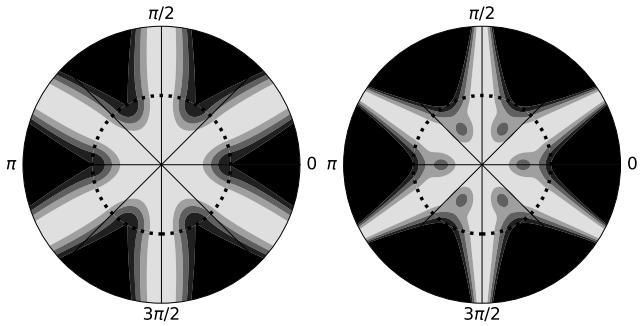

FIG. 8: The probability density $|\psi_n(\mathbf{r})|^2$ for $m = 3$ and $V_0 = 10$, for the first $q_i = 1$ [left panel] and second $q_i = 2$ [right panel] internal resonances, see Fig. 4b, flows $q_i = 1, 2$. High (low) density shown as dark (light). Black dotted ring at $r = 1$ is well boundary.

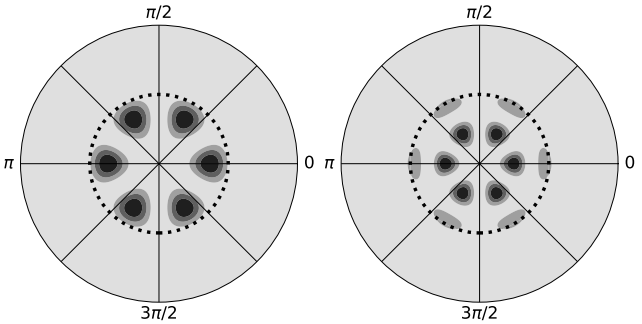

FIG. 9: The probability density $|\psi_n(\mathbf{r})|^2$ for the ground [left panel] and first excited [right panel] bound states with $m = 3$ and $V_0 = 80$, see positive imaginary axis of Fig. 4b. High (low) density shown as dark (light). Black dotted ring at $r = 1$ is well boundary.

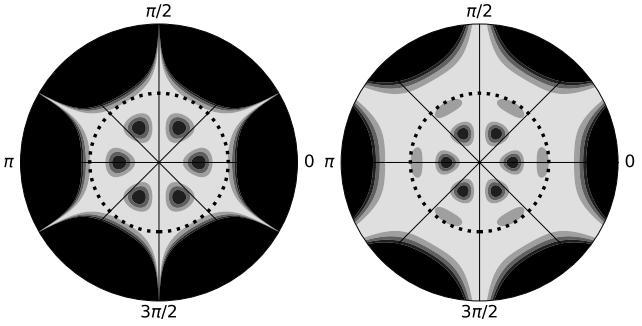

FIG. 10: The probability density $|\psi_n(\mathbf{r})|^2$ for the first [left panel] and second [right panel] quasi antibound states with $m = 3$ and $V_0 = 80$, see black colored flows in Fig. 4b. High (low) density shown as dark (light). Black dotted ring at $r = 1$ is well boundary.

symmetry is present in this case, however more work is needed to explain how this is consistent with state conservation. The anomalous behavior here is a reflection of the absence of modified Hankel function zeros for $m = 0$.

With reference to the somewhat similar optical problem discussed in Ref. [10], the flows of internal resonances in that work go to zeros of Bessel functions on the real axis in the small opening limit $n \to \infty$, where n is the refractive index of a 2D microdisk, and no bound states are produced. Moreover, there are no spirals for the external resonances.

When polar density maps of the eigensolutions are plotted, the characteristic field pattern of whispering gallery modes (WGMs) becomes apparent. For particular values of m, there are $2m$ "hot spots" in the azimuthal direction, as expected for such modes. For fixed m, there are increasing numbers of hot spots in the radial direction as the radial modal index q_i is increased. The case $m = 3$ was chosen as a representative example for which to show wavefunctions, since it encapsulates all features observed for other values of m. The resulting plots are shown in Figs. 7 - 10. The bound states have the expected density characteristics - the wave function exists almost entirely inside the potential. Quasi antibound states resemble bound states inside the potential, but diverge outside the well. The field plots of the resonances are the most interesting. The plots are highly sensitive to both potential depth and the magnitude of the imaginary part of the wavenumber.

V. CONCLUSIONS

The numerical solution of the time independent Schrodinger equation for various simple potentials is now a common and vastly simplified endeavor given the power of modern computers, and the availability of mathematical software. It is surprising that such rich dynamics emerges for what is, after all, a simple two dimensional symmetric potential. We expect that a similar, and perhaps even more profound response might be observed for other relatively simple potentials, and this will be investigated in due course. The remaining question here, however, relates to degeneracy and the issue of state conservation. This will be addressed in future work by destroying the symmetry of the potential by placing point-

like defects inside the well, and also by distorting the geometry of the potential itself. These methods will lift the degeneracy of the states, and will likely precipitate even more intriguing flow dynamics.

[1] H. M. Nussenzveig, Nucl. Phys. **11**, 499 (1959).
[2] D. W. L. Sprung, H. Wu, and J. Martorell, Am. J. Phys. **64**, 136 (1996).
[3] R. Zavin and N. Moiseyev, J. Phys. A: Math. Gen. **37**, 4619 (2004).
[4] B. Belchev, S. G. Neale, and M. A. Walton, Can. J. Phys. **89**, 1127 (2011).
[5] A. Tanimu and E. A. Muljarov, Phys. Rev. A **98**, 22127 (2018).
[6] R. W. Robinett, Am. J. Phys. **64**, 440 (1996).
[7] R. W. Robinett and S. Heppelmann, Phys. Rev. A **65**, 062103 (2002).
[8] R. Dubertrand, E. Bogomolny, N. Djellali, M. Lebental, and C. Schmit, Phys. Rev. A **77**, 013804 (2008).
[9] E. Bogomolny, R. Dubertrand, and C. Schmit, Phys. Rev. E **78**, 056202 (2008).
[10] C. P. Dettmann, G. V. Morozov, M. Sieber, and H. Waalkens, EPL **87**, 34003 (2009).
[11] J. Cho, I. Kim, S. R. G.-S. Yim, and C.-M. Kim, Phys. Lett. A **374**, 1893 (2010).
[12] J. Cho, S. Rim, and C.-M. Kim, Phys. Rev. A **83**, 043810 (2011).
[13] H. Cao and J. Wiersig, Rev. Mod. Phys. **87**, 61 (2015).
[14] N. Michel, W. Nazarewicz, M. Ploszajczak, and J. Rotureau, Phys. Rev. C **74**, 054305 (2006).
[15] C. P. Dettmann, G. V. Morozov, M. Sieber, and H. Waalkens, Phys. Rev. A **80**, 063813 (2009).
[16] M. Abramowitz and I. A. Stegun, *Handbook of Mathematical Functions* (US Govt., 1972).
[17] I. S. Gradshteyn and I. M. Ryzhik, *Tables of Integrals, Series, and Products* (Academic Press, 2007).
[18] M. B. Doost, W. Langbein, and E. A. Muljarov, Phys. Rev. A **87**, 043827 (2013).
[19] A. Cruz and J. Sesma, Math. Comp. **39**, 639 (1982).
[20] M. K. Kerimov and S. L. Skorokhodov, Comput. Maths. Math. Phys. **25**, 26 (1985).
[21] A. Erdelyi, *Higher Transcendential Functions, Vol. II* (McGraw-Hill, New-York, 1953).
[22] S. Wagon, *Mathematica in Action* (Springer-Verlag, New York, 2010).